

Assessing safety conditions in underground excavations after a methane-air mixture explosion

*Mykola Nalisko*¹, *Valerii Sobolev*², *Dmytro Rudakov*^{*3}, and *Nataliia Bilan*⁴

¹Prydniprovsk State Academy of Civil Engineering and Architecture, Department of Health and Safety, 24a Chernyshevskoho St., 49600 Dnipro, Ukraine

²Dnipro University of Technology, Department of Construction, Geotechnics and Geomechanics, 19 Yavornytskoho Ave., 49005 Dnipro, Ukraine

³Dnipro University of Technology, Department of Hydrogeology and Engineering Geology, 19 Yavornytskoho Ave., 49005 Dnipro, Ukraine

⁴Dnipro University of Technology, Department of General and Structural Geology, 19 Yavornytskoho Ave., 49005 Dnipro, Ukraine

Abstract. A technique for evaluation of shock wave impulse after a methane-air mixture explosion is elaborated. The numerical model developed in previous studies has been verified in the laboratory by using laser initiation of explosives and measuring the pressure impulses of explosion products on a ballistic pendulum. To evaluate the mechanical impulse the functional correlations between its magnitude, the swing angle, and the pendulum characteristics have been derived analytically. The reliability of experimental results is ensured by calibrating the sensor that measures the pendulum swing angle and estimating the impulse measurement errors caused by specifics of angle measurements by a digital voltmeter, pendulum axis friction, and the pauses between measurements. Testing the developed technique to evaluate the shock wave impact showed satisfactory consistency of experimental and theoretical results with the momentum deviation below 9%, which confirms model applicability and correct reproducibility of the shock wave propagation process.

1 Introduction

The explosion of a methane-air mixture in an underground coal mine excavation is considered as one of the most dangerous catastrophic events in mining [1, 2]. The specifics of methane-air and/or dust-air mixture explosions consist in generation of shock waves and their propagation through the mine excavation network [3 – 6]. The shock wave (SW) is believed to be the main factor threatening the life and health of miners, leading to excavation collapses and damage of mining equipment operated underground.

Many experts suggested the ambiguous nature of the source that initiates the ignition and explosion of the methane-air mixture [7, 8]. In general, the explosions may be triggered

* Corresponding author: rudakov.d.v@nmu.one

by the human factor, geological settings, and gassiness of coal seams. The changes in technologies, equipment operation mode, the physicochemical properties of coal being destructed due to nanostructure stability violation, etc. can also initiate gas-dynamic phenomena [9 – 13]. However, the most probable causes of changing the aforementioned factors under their mutual influence still remain unknown. At the same time, recent studies using numerical modelling demonstrated notable achievements [14 – 16]; the proposed ideas and obtained results will be taken into account in this study.

The experience of rescue operations in emergency areas of coal mines demonstrated that repeated explosions in the underground atmosphere that occur in disconnected zones separated by the barriers are of particular concern. This is evidenced by the destruction of blast-resistant structures after gas explosions in such zones and generation of high pressure SWs dangerous to humans and damaging blast door defences for the personnel despite keeping safe distances evaluated by all existing methods. For example, two explosions occurred in such zones at the mine named after O.F. Zasiadko in 2008 resulted in the destruction of blast door defences and the death of rescuers. Under these conditions, the SW parameters in underground excavations should be predicted with the sufficient accuracy that guarantees the safety of mining operations and stability of protective barriers mitigating the destructive SW impact.

The explosions of methane-air mixtures in coal mines or gas-air mixtures in the enterprises using explosives are the topical labour safety problem. Latest technological accidents in Ukraine and abroad showed that emergencies and their consequences pose at least the same and often direct threat to fire-fighters and rescuers. Of course, the complete elimination of accidental explosion risks is now impossible; but evaluation of reliable ranges for the SW impact on blast-resistant barriers is a realistic task of high importance. Addressing this problem would allow assessing the safety conditions in the aftermath of accidents and evaluating blast resistance capacity of shelters and other constructions [1, 2].

The mechanical impulse of SWs has the major impact on blast-resistant constructions. Studying and predictive calculation of this impulse is believed to be one of the most difficult problems of gas dynamics due to rapid changes of time-dependent parameters, multiple wave front propagation, the lack of universal devices and sensors to directly measure the explosion impulses. This greatly complicates the research and enforces to focus on theoretical studies making a number of simplifying assumptions and hypotheses that have to be verified experimentally.

For experimental studying the SW impulse in underground excavations a device has been developed to allow making measurements for successive short-delay explosive charges generating multi-front shock waves with the deviation from theoretical results below 23% [17]. The numerical results of overpressure evolution during the explosions in gas furnaces were compared with the results of physical modelling the explosion in a pilot plant of combustion chamber geometry. Conversely, analytical calculation results were experimentally verified.

A numerical solution to the system of gas dynamic equations proposed in [18] enabled calculating the dynamic load on blast-resistant constructions. Besides, the criteria for comparing the results of numerical modelling with analytical solutions and experimental measurements have been justified; they allowed identifying the consistency of numerical modelling [19, 20].

To evaluate the dynamic load on blast-resistant shelters in underground excavations a numerical technique of large particles based on gas dynamics theory has been developed [21 – 23]. It allows calculating the SW impulse by integrating the overpressure emerging in the plane of the rigid wall for the period of time when this overpressure exists:

$$I = \int_0^{t_e} (P(t) - P_0) dt, \quad (1)$$

where I is the force action impulse, Pa·s; t_e the time period when the overpressure exists, s; $P(t)$ the pressure emerging on the unit surface of a blast-resistant construction, Pa; t time, s; P_0 the initial pressure, Pa.

This study aims to verify the developed method of SW impulse calculation by comparing to a physical experiment, which makes possible assessing the reliability of the numerical model proposed for prediction of the underground methane-air explosion impact.

2 Materials and methods

In this study, the pressure impulse was measured using the method of ballistic pendulum due to its reliability, measurement accuracy and ease of implementation (Fig. 1), with the impulse being calculated based on the swing angle.

Impulse transfer to the pendulum was theoretically justified by K.P. Stanyukovich's solutions to the boundary value problem of dispersion of the gases generated at an instantaneous detonation [24], which allows calculating the momentum density as:

$$J_s = \xi \sqrt{2m_s E_s}, \quad (2)$$

where m_s is the explosive mass per unit of surface area (mass density); E_s the internal energy of detonation products falling per unit of surface area (energy density); ξ the proportionality factor depending on the adiabatic index of detonation products.

Internal energy E_s is assumed to be proportional to the energy Q of chemical transformation under constant volume.

To meet the conditions of this process in physical modelling an explosion of a condensed charge able to volume detonation and being in contact with the barrier has to be reproduced at the end of the ballistic pendulum. In this case the surge overpressure in the barrier plane emerges right in a gaseous medium i.e. in detonation products, which fully meets the conditions of gas explosion. The same conditions on the contact with the barrier (fuel-air explosion) are modelled by setting the initial gas mixture temperature in the computational domain equal to the gas self-ignition temperature.

To reproduce the volume igniting in a physical experiment the laser technique for explosive charge initiation is proposed [25 – 28]. Optically transparent moderated lead azide $Pb(N_3)_2$ embedded in a polymer matrix as the micro-crystals has been used as an explosive. A chemical reaction was activated by heating the optical micro-irregularities in the laser beam focus, which ensures volumetric explosion [29 – 32].

The criteria of energy and geometrical similarity were used to keep the identity between the experiment and the numerical model. The geometrical similarity criterion Π_g is satisfied for the area to which the energy impulse is transferred; the energy similarity criterion Π_e is satisfied for the surface density of internal energy:

$$\Pi_g = \frac{d_e}{d_c} = 1, \quad \Pi_e = \frac{E_{s,e}}{E_{s,c}} = 1, \quad (3)$$

where d_e and d_c are the diameter of a circle coated with an explosive layer in the experiment and the diameter of the rigid barrier in a 2D calculation domain, respectively; $E_{s,e}$ and $E_{s,c}$ the internal energy of chemical transformation in the experiment and in the calculation domain, respectively.

A SW impulse in the experiment was reproduced by using a sample of moderated lead azide deposited on the aluminium foil. The specific surface density of the coated sample $m_s = 30 \text{ mg/cm}^2$, the diameter of spraying $d_e = 1 \text{ cm}$. Chemical transformation energy of lead azide is 1.536 MJ/kg; therefore, the specific surface energy density reaches 46 J/cm^2 ,

and the surface energy density per impulse transfer area $E_{s,c}$ makes 35.325 J.

To evaluate the surface energy density in the computation domain similar to that in the experiment we evaluated the mass of the methane-air mixture (9% of the volume) and the length of the computational domain filled with the gas (Figs. 1 and 2).

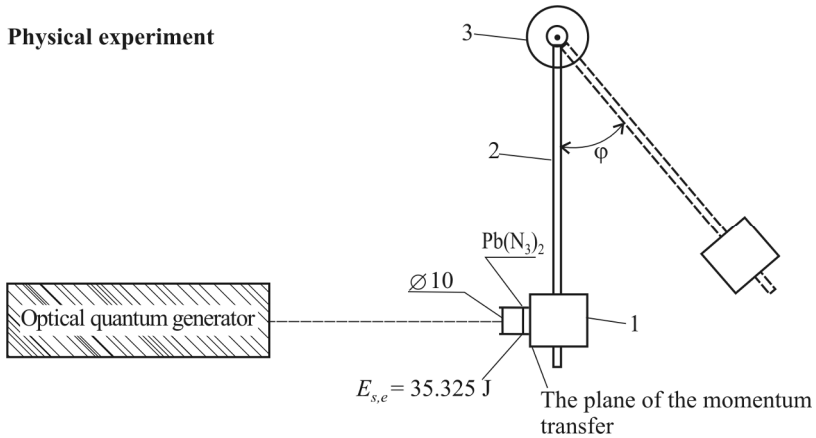


Fig. 1. Sketch of a physical domain: 1 – metal disk, 2 – thin-walled tube, 3 – resistor.

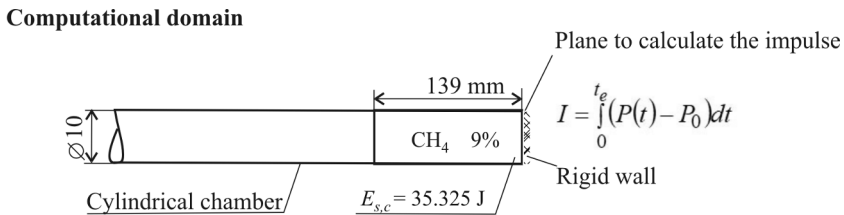


Fig. 2. Sketch of a computational domain.

The methane oxidation energy is 50.4 MJ/kg; by applying stoichiometric methane concentration of 5.5% we estimated the methane-air mixture oxidation energy at 2.75 MJ/kg. The mass of reactive mixture with a surface energy density for a volume of 10.9 cm^3 equals to 12.8 g at the same surface energy $E_{s,c} = 35.325 \text{ J}$ as in the experiment. The thickness of the methane-air mixture layer near the rigid wall of the cylindrical channel with a diameter of 1 cm and the mixture density of 1.17 g/cm^3 equals to 13.9 cm.

The experimental setup has been designed based on the solid-state optical quantum oscillator of neodymium glass. The setup includes the optical system to initiate the explosive and the measurement devices (Fig. 3).

The sample of explosives δ in the form of a circle with the diameter 1.0 cm made of aluminium foil of 0.1 mm thickness coated with moderated lead azide was fastened to pendulum base 5. The pendulum with deviation angle sensor 7 was placed in blasting chamber 4.

The pendulum was designed in such a way (Fig. 4) to ensure impulse measurement in the range of swing angles from 10° to 50° . Metal disc 3 was mounted on a long thin tube 2; one of its ends was rigidly fixed to the axis of the variable wireless resistor 1 providing linear correlation between the resistance and the rotation angle of the movable contact.

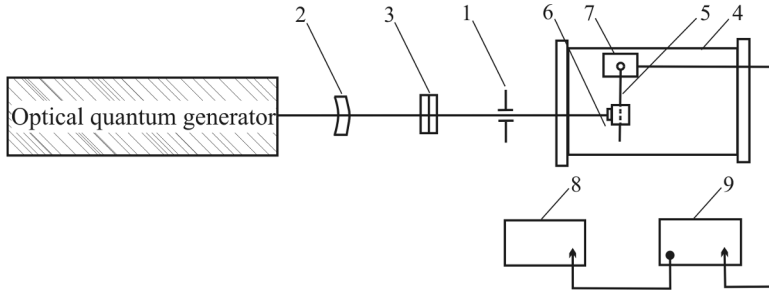


Fig. 3. Sketch of the experimental setup: 1 – aperture, 2 – lenses, 3 – filters, 4 – blasting chamber, 5 – pendulum, 6 – sample of explosives, 7 – pendulum swing angle, 8 – digital voltmeter, 9 – memory.

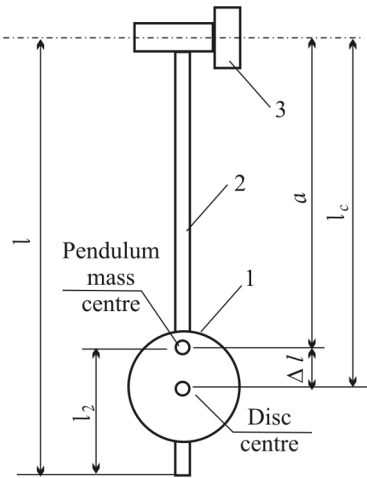


Fig. 4. Sketch of the ballistic pendulum: 1 – pendulum disk, 2 – thin-walled tube, 3 – resistor.

A thin-walled steel pipe of the length $l = 35.0$ cm and a mass per length unit $\rho = 0.175$ g/cm was fixed to the pendulum disc. To evaluate the range of impulses measurable by the available disk of mass $m_d = 31.38$ g we derived a formula that correlates the magnitude and swing angle.

3 Results and discussion

Regarding to the short-term period of the explosion product impacts on the pendulum (shorter than 10^{-5} s), we can assume that the pendulum gains an impulse when the swing angle ϕ equals to zero. In this case, the conservation energy law can be written as:

$$E_m = E_p, \quad (4)$$

where E_m is the energy transferred to the pendulum by explosion products, E_p the potential energy of the raised or deviated pendulum. This equation can be rewritten as:

$$\frac{M v_0^2}{2} = Mg a - Mg a \cos \phi, \quad (5)$$

where $M = m_d + m_t$ is the pendulum mass, m_d the disc mass, m_t the tube mass; g the gravity

acceleration; a the distance from the suspension point to the mass centre; φ the pendulum swing angle.

Equation (5) is derived from the mathematical pendulum equation by replacing the length l in the right hand side with the distance a . Based on equation (5) we can express the function relating the gained pendulum momentum and the swing angle as follows:

$$J = 2M\sqrt{ga} \sin \frac{\varphi}{2}. \quad (6)$$

Then, the momentum density is calculated as:

$$J_s = \frac{2M}{S} \sqrt{ga} \sin \frac{\varphi}{2}, \quad (7)$$

where S is the area to which the momentum is transferred.

To calculate the impulse by equation (7) we derived the distance a between the suspension point and the pendulum mass centre using the system of equations (notations see in Fig. 4):

$$\begin{cases} l = a + l_2; \\ l_c = a + \Delta l; \\ \frac{\rho a^2}{2} = \frac{\rho l_2^2}{2} + m_d \Delta l. \end{cases} \quad (8)$$

The last expression in equation (8) is the momentum force equality with respect to the mass centre. It is derived assuming that the pendulum mass centre is located between two segments; the first one is the pendulum tube with the lever of the length a , the second one is the pendulum tube with the lever of the length l_2 and a disc with a lever of the length Δl (Fig. 3). Solving the system of equations (8) with respect to the parameter a we obtained:

$$a = \frac{l m_c + 2l_c m_d}{2M}. \quad (9)$$

To avoid additional momentums when loading the pendulum that may cause calculation errors the centre of the momentum transfer area should coincide with the axis of the pendulum centre mass. In the experiments, a disc of the mass that just 5 times exceeds the mass of the rod has been used. Preliminary calculations showed that if the disc would be mounted at the end of the rod, the pendulum mass centre would go beyond the disc radius limits ($r_d = 1$ cm). Therefore, to align the mass centre with the disc centre, the latter was positioned at the rod centre, i.e. at the distance $l_c = 17.5$ cm from the pendulum rotation axis. Taking into account that $m_s = 0.175 \cdot 35.0 = 6.13$ g, we find the range for measuring the density impulse for this disc and the angle range from 10° to 50° :

$$\begin{aligned} m_d &= 0.03138 \text{ kg}; \quad M = 0.03751 \text{ kg}; \quad a = l_c = 0.175 \text{ m}; \\ J &= (0.110 - 0.526) \text{ kPa}\cdot\text{s}. \end{aligned} \quad (10)$$

To measure the pendulum angle directly we used the unbalanced bridge circuit that evaluated the angle change by indications of the gage in the measuring circuit. The power supply was connected to another bridge circuit.

Functioning the gage and recording the data were synchronized with laser performance by the device that started recording the data simultaneously with the lighting up of the laser pump lamp and was disconnected periodically after a specified time interval.

The accuracy of the pendulum swing angle was evaluated after calibrating the circuit of sensors that measured the angle φ varied within the range from 5° to 85° with the increments of 5° .

The conversion factor was determined by the expression:

$$k = \frac{U}{\varphi}, \quad (11)$$

where U is the measured voltage. The average value for the conversion factor k of 0.0434 was evaluated based on averaging the calibration results.

The total measurement error of the impulse can be calculated as:

$$\gamma_\Sigma = \tilde{\gamma}_U + \tilde{\gamma}_f + \tilde{\gamma}_\tau, \quad (12)$$

where $\tilde{\gamma}_U$ is the error caused by the specifics of voltmeter measurement, $\tilde{\gamma}_f$ the error caused by the friction force, $\tilde{\gamma}_\tau$ the error caused by the pause between measurements.

The error caused by the specifics of measurement by the voltmeter integrated in the unbalanced bridge circuit was evaluated as the ratio of the absolute voltage error ΔU to the measured voltage U in percent:

$$\gamma_U = \frac{\Delta U}{U} 100\%. \quad (13)$$

The value of ΔU was evaluated using the standard method as the result of calibrating the sensor that measures the swing angle.

The error in impulse evaluation associated with the inaccuracy of electrical measurements is determined by the formula:

$$\tilde{\gamma}_U = \frac{\Delta J}{J} \gamma_U. \quad (14)$$

The difference ΔJ was derived as the differential of the function J at $\varphi = \varphi_0$ assuming $\Delta\varphi \rightarrow 0$. In this case:

$$\tilde{\gamma}_U = \frac{\varphi_0}{2} \cot\left(\frac{\varphi_0}{2}\right) \gamma_U. \quad (15)$$

Substituting the pendulum deflection angle $\varphi_0 = 5^\circ$ to equation (15) we obtain $\tilde{\gamma}_U \approx 4.7\%$.

The error caused by the friction force leads to an underestimation of the maximum swing angle. To estimate the swing angle φ we consider the governing equation of pendulum motion:

$$\varphi'' + 2\lambda\varphi' + \omega_0^2\varphi = 0, \quad (16)$$

where ω_0 is the cyclic (Eigen) frequency of free continuous pendulum oscillations at $\lambda = 0$ in the absence of energy losses, $\omega_0^2 = g/l$, λ the oscillation attenuation rate, $2\lambda = \mu/(Ml)$, μ the friction coefficient.

Assuming that $\varphi = 0$ at $t = 0$ we found the time-dependent solution of equation (16):

$$\varphi_f(t) = A e^{-\lambda t} \sin \omega t, \quad (17)$$

where φ_f is the pendulum angle calculated with the friction; $\omega = \sqrt{\omega_0^2 - \lambda^2}$, A the constant.

The error caused by the friction force can be calculated by the formula:

$$\gamma_f = \frac{\varphi - \varphi_f}{\varphi_f} 100\% = \frac{1 - \exp(-\lambda T_p / 4)}{\exp(-\lambda T_p / 4)} 100\%, \quad (18)$$

where $\varphi = A \sin \omega t$ is the pendulum angle defined without the friction effect; T_p the pendulum period.

The error of impulse measurement associated with the friction effect is calculated by the formula:

$$\tilde{\gamma}_f = \frac{\Delta J}{J} \gamma_f = \frac{\varphi_0}{2} \cot\left(\frac{\varphi_0}{2}\right) \gamma_f. \quad (19)$$

Substituting the pendulum parameter to equation (19) we obtained $\tilde{\gamma}_f = 2.34\%$.

The error caused by the pause between measurements. The digital voltmeter in the laboratory setup records the data at the frequency of 25 Hz, which allows measuring the swing angle every 40 ms, thus, determine the time-dependent function $\varphi(t)$ as a time series. Numerical analysis of $\varphi(t)$ enables calculating the oscillation attenuation rate. The maximum error of evaluating the angle φ due to the pause between two successive measurements of the pendulum position equals to the angle by which the pendulum deviates in a position close to the maximum deviation in time $\tau/2$ where τ is the time between the measurements. The error of measuring the angle caused by this factor is evaluated by the formula:

$$\gamma_\tau = \frac{\Delta\varphi}{\varphi_0} 100\%. \quad (20)$$

The deviation $\Delta\varphi$ is calculated as the difference between the actual and recorded angles:

$$\Delta\varphi = A \sin\left(\omega \frac{T_p}{4}\right) - A \sin\left[\omega \left(\frac{T_p}{4} \pm \frac{\tau}{2}\right)\right] = A \sin\left(\frac{\omega T_p}{4}\right) - A \sin\left(\frac{\omega T_p}{4} \pm \frac{\omega \tau}{2}\right), \quad (21)$$

Solving equation (21) we obtained:

$$\gamma_\tau = \frac{1}{2} \left(\frac{\omega \tau}{2}\right)^2 100\%. \quad (22)$$

Substituting $\omega = 2\pi/T_p$, $T_p = 1.28$ s, $\tau = 0.04$, $\varphi_0 = 5^\circ$ we evaluated the relative error caused by the pause between measurements:

$$\tilde{\gamma}_\tau = \frac{\Delta J}{J} \gamma_\tau = \frac{\varphi_0}{2} \cot\left(\frac{\varphi_0}{2}\right) \gamma_\tau = 0.998 \cdot 0.481 = 0.48\%. \quad (23)$$

Summarizing the results of error estimations (see equations (15), (19), and (23)) we can estimate the total measurement error of the impulse evaluation using the pendulum according to equation (12):

$$\gamma_\Sigma = \tilde{\gamma}_U + \tilde{\gamma}_f + \tilde{\gamma}_\tau = 4.7\% + 2.35\% + 0.48\% = 7.53\%,$$

that is satisfactory for practical needs.

In the experiment, we used the samples made of moderated lead azide manufactured according to the technology described in [27 – 29]. The surface mass density of the samples was controlled using an analytical balance; it varied at $m_s = 30$ mg/cm² with the maximum

deviation of 5 mg/cm^2 . Accordingly, the volume of the methane-air mixture was estimated in the numerical model. In total, 5 experiments have been conducted (Table 1). In Table 1 ρ_1 is the explosive surface density of the sample, m_{PbN} the mass of lead azide sample, φ the pendulum swing angle, J_m the momentum density measured (see equation (7)), J_c the momentum density calculated, δ the relative deviation.

The numerical model reproduced the explosion of the methane-air mixture in a cylindrical channel, with one of its ends being closed by a rigid wall and the opposite end being open. The methane-air mixture was assumed to be concentrated at the closed end. The computational grid size was set of 10^{-3} m at the time step was $0.1 \mu\text{s}$, which allowed detailed investigating all process phases including the start of combustion, transition to detonation, gas flow and SW front propagation.

Table 1. Comparison of experimental and calculation results
(arranged by increasing the mass of explosive m_{PbN}).

Experiment nr.	$\rho_1, \text{ mg/cm}^2$	$m_{PbN}, \text{ mg}$	$\varphi, \text{ grad.}$	$J_m, \text{ kPa}\cdot\text{s}$	$J_c, \text{ kPa}\cdot\text{s}$	$\delta, \%$
5	25.5	20.0	23.6 \pm 1.7	0.256	0.263	-2.7
3	26.2	20.6	24.3 \pm 1.8	0.263	0.247	6.4
1	30.0	23.5	27.7 \pm 2.0	0.300	0.270	9.0
2	32.5	25.5	30.0 \pm 2.2	0.324	0.305	6.2
4	33.7	26.5	31.2 \pm 2.3	0.337	0.354	-5.0

The maximum relative deviation δ between the measured in the laboratory and calculated SW impulses does not exceed 9%, which is sufficient for practical needs. Regarding to the low deviation between theoretical and experimental results, the developed numerical method can be used to predict the SW force impact on blast door defences in underground excavations, which is of high importance for assessing the safety of mine rescuers and the personnel under the threat of emergency explosions.

4 Conclusions

The proposed method for experimental measurement of pressure impulses generated by the explosion products, combining the ballistic pendulum with the technology of laser initiation of photosensitive explosives, allows verifying the numerical methods applied to predict the explosion load on blast-resistant constructions. The correctness of the theoretical model and its reproducibility of the real physical process enable assessing the safety conditions for rescuers involved in the responses to accidents in coal mines.

The authors are grateful to the managers of the Pavlohrad chemical plant, especially to Director-General, Corr. National Academy of Sciences of Ukraine L.M. Shyman, Technical Director, Dr. of Technical Sciences Ye.B. Ustymenko, Deputy director in Research, L.I. Pidkamenna, for the opportunity to use an explosive site and support in conducting the experiments. The work is funded by the Ministry of Education and Science of Ukraine (Order Nr. 199 on February 10, 2017).

References

1. Karaush, S.A. (2014). *Otsenka parametrov promyshlennykh vzryvov*. Tomsk: TGASU.
2. Stoetsky, V.F., Golinko, V.I., & Dranishnikov L.V. (2014). Risk assessment in man-caused accidents. *Naukovyi Visnyk Natsionalnoho Hirnychoho Universytetu*, (3), 117-125.
3. Izmailov, A.V., Romanchenko, S.B., Podobrazhin, S.N., Rudenko, Yu.F., & Kosterenko, V.N. (2004). Sostoyanie bezopasnosti v ugol'noy otrasli i puti ee povysheniya na sovremennom etape. *Gornaya Promyshlennost'*, (5), 16-21.

4. Abinov, A.G., Mitrofanov, V.P., & Chekhovskikh, A.M. (1976). Detonatsiya metanopylevozdushnoy smesi v gornyykh vyrabotkakh shakht. *Tekhnika Bezopasnosti, Okhrana Truda i Gornospasatelnoe Delo*, (10), 10.
5. Bykov, A.M., & Prozorov, A.N. (1980). Vozmozhnost' vozniknoveniya sil'nykh vzryvov ugol'noy pyli v tupikovyykh vyrabotkakh nebol'shoy protyazhennosti. *Fizika Goreniya i Vzryva*, (1), 153-154.
6. Plotnikov, V.M. (1992). Obespechivaetsya li bezopasnost' truda gornospasateley pri ugroze vzryva gaza i pyli v ugol'nykh shakhtakh. *Bezopasnost' Truda v Promyshlennosti*, (1), 29-33.
7. Skritskiy, V.A. (2006). Vzryvy metanovozdushnoy smesi v ugol'nykh shakhtakh Kuzbassa. Prichiny i sposoby ikh predotvrashcheniya. *Gornaya Promyshlennost'*, (4), 78.
8. Grechikhin, L.I., Shevtsov, N.R., Kunenko, I.V., & Kuts, N.G. (2014). Fizika goreniya i vzryva metanovozdushnoy smesi i ugol'noy pyli. *Naukovi Pratsi Donetskoho Natsionalnoho Tekhnichnoho Universytetu*, (1), 104-111.
9. Khomenko, O., Kononenko, M., & Myronova, I. (2017). Ecological and technological aspects of iron-ore underground mining. *Mining of Mineral Deposits*, 11(2), 59-67. <https://doi.org/10.15407/mining11.02.059>
10. Khomenko, O., Kononenko, M., & Bilegsaikhan, J. (2018). Classification of Theories about Rock Pressure. *Solid State Phenomena*, (277), 157-167. <https://doi.org/10.4028/www.scientific.net/SSP.277.157>
11. Rudakov, D. & Sobolev, V. (2019). A mathematical model of gas flow during coal outburst initiation. *International Journal of Mining Science and Technology*, 29(3). <https://doi.org/10.1016/j.ijmst.2019.02.002>
12. Khomenko, O., Kononenko, M., Kovalenko, I., & Astafiev, D. (2018). Self-regulating roof-bolting with the rock pressure energy use. *E3S Web of Conferences*, (60), 00009. <https://doi.org/10.1051/e3sconf/20186000009>
13. Soboliev, V., Bilan, N., & Kirichenko, O. (2014). Mechanism of additional noxious fumes formation when conducting blasting operations in rock mass. *Progressive Technologies of Coal, Coalbed Methane, and Ores Mining*, 471-477. <https://doi.org/10.1201/b17547-41>
14. Vasenin, I.M., Paleev, D.Yu., Rudenko, Yu.F., Kosterenko, V.N., Kraynov, A.Yu., Lukashov, O.Yu., & Shrager, E.R. (2008). O matematicheskikh modelyakh vzryva (vspyshki) v gornyykh vyrabotkakh ugol'nykh shakht. *Izvestiya Vuzov. Fizika*, 51(8), 95-100.
15. Ageev, V.G., Grekov, S.P., Zinchenko, I.N. & Salakhutdinov, T.G. (2013). Komp'yuternoe modelirovanie razvitiya, rasprostraneniya i lokalizatsii vzryvov metanovozdushnykh smesey v gornyykh vyrabotkakh. *Visnyk Kharkivskoho Natsionalnoho Universytetu*, (1058), 5-12.
16. Sobolev, V.V., Nalis'ko, N.N., & Bartashevskaya, L.I. (2018). Parametry makrokinetiki goreniya uglevodorodov v chislennom raschete avariynykh vzryvov v gornyykh vyrabotkakh. In *Forum Hirnykiv* (pp. 72-83). Dnipro, Ukraine: Natsionalnyi hirnychiy universytet.
17. Russkikh, V.V., Yavorskiy, A.V., & Yavorskaya, Ye.A. (2012). *Parametry vzryvozashchitnykh ustroystv dlya gasheniya udarnykh vozdushnykh voln pri podzemnoy dobyche rud*. Dnipropetrovsk: Natsionalnyi hirnychiy universytet.
18. Barg, M.A., & Polandov, Yu.Kh. (2008). O modelirovanii rasprostraneniya plameni v zamknutom tsilindricheskom kanale. *Izvestia Orel State Technical University. Series Fundamental and Applied Problems of Engineering and Technology*, 1-2/269(544), 30-32.
19. Belyaev, N.N., & Karpov, A.A. (2015). Zashchita okruzhayushchey sredy pry transportirovke uglya. *Zbirnyk Naukovukh Prats Natsionalnoho Hirnychoho Universytetu*, (48), 223-228.
20. Vorob'yev, V.V., & Pomazan, M.V. (2014). O vliyaniy konstruktssii zaryada na kharakter razvitiya nachal'noy stadii razrusheniya tverdykh sred. *Visnyk Kremenchutskoho Natsionalnoho Universytetu imeni Mykhaila Ostrohradskoho*, (1), 124-129.
21. Nalis'ko, N.N. (2013). Chislennyy raschet dinamicheskoy nagruzki ot vozdeystviya vozdushnykh udarnykh voln na inzhenernye sooruzheniya. In *Vysokoenergeticheskie Sistemy, Protssy i ikh Modeli* (pp. 255-266). Dnipropetrovsk, Ukraine: Aktsent PP.

22. Nalis'ko, N.N. (2013). Gazodinamicheskiy raschet parametrov rasprostraneniya vozdushnykh udarnykh voln v gornyykh vyrabotkakh. *Visnyk Kremenchutskoho Natsionalnoho Universytetu imeni Mykhaila Ostrohradskoho*, (5), 136-144.
23. Nalis'ko, N.N., & Chernay, A.V. (2013). Obosnovanie novykh podkhodov k raschetu parametrov vzryvnogo gorennya gazovozdushnykh smesey v vyrabotkakh ugol'nykh shakht. In *Vysokoenergeticheskie Sistemy, Protsessy i ikh Modeli* (pp. 267-278). Dnipropetrovsk, Ukraine: Aktsent PP.
24. Stanyukovich, K.P. (1971). *Neustanovivshiesya dvizheniya sploshnoy sredy*. Moskva: Nauka.
25. Sobolev, V.V., Ustimenko, Ye.B., Nalisko, M.M., & Kovalenko, I.L. (2018) The macrokinetics parameters of the hydrocarbons combustion in the numerical calculation of accidental explosions in mines. *Naukovyi Visnyk Natsionalnoho Hirnychoho Universytetu*, (1), 89-98. <https://doi.org/10.29202/nvngu/2018-1/8>
26. Chernaj, A.V., Sobolev, V.V., Ilyushin, M.A., & Zhitnik, N.E. The method of obtaining mechanical loading pulses based on a laser initiation of explosion of explosive coatings. *Fizika Gorennya i Vzryva*, 30(2), 106-111.
27. Chernaj, A.V., Sobolev, V.V., Ilyushin, M.A., & Zhitnik, N.E. (1994). Generating mechanical pulses by the laser blasting of explosive coating. *Combustion, Explosion, and Shock Waves*, 30(2), 239-242. <https://doi.org/10.1007/BF00786134>
28. Chernaj, A.V., & Sobolev, V.V. (1995). Laser method of profiled detonation wave generation for explosion treatment of materials. *Fizika i Khimiya Obrabotki Materialov*, (5), 120-123.
29. Chernaj, A.V., Sobolev, V.V., Ilyushin, M.A., Zhitnev, N.E., & Petrova, N.A. (1996). On the mechanism of ignition of energetic materials by a laser pulse. *Chemical Physics Reports*, 15(3), 457-462.
30. Chernaj, A.V., Sobolev, V.V., Chernaj, V.A., Ilyushin, M.A., & Dlugashek, A. (2003). Laser initiation of charges on the basis of di-(3-hydrazino-4-amino-1, 2, 3-triazol)-copper (II) perchlorate. *Fizika Gorennya i Vzryva*, 39(3), 105-110.
31. Sobolev, V. V., & Usherenko, S. M. (2006). Shock-wave initiation of nuclear transmutation of chemical elements. *Journal de Physique IV (Proceedings)*, (134), 977-982. <https://doi.org/10.1051/jp4:2006134149>
32. Chernaj, A.V., Sobolev, V.V., Chernaj, V.A., Ilyushin, M.A., & Dlugashek, A. (2003). Laser ignition of explosive compositions based on di-(3-hydrazino-4-amino-1,2,3-triazole)-copper(II) perchlorate. *Combustion, Explosion and Shock Waves*, 39 (3), 335-339. <https://doi.org/10.1023/A:1023852505414>